First-Principles Identification of Iodine Exchange Mechanism in Iodide Ionic Liquid

2 AUTHORS, INCLUDING:

Letter

# First-Principles Identification of Iodine Exchange Mechanism in Iodide Ionic Liquid

Ranjit Thapa and Noejung Park*

Interdisciplinary School of Green Energy, Ulsan National Institute of Science and Technology, Ulsan 689-798, Republic of Korea

S *Supporting Information*

ABSTRACT: We investigated the microscopic mechanism of ion transport in iodide ionic liquid, using first-principles calculations. We show that the desorption barrier of polyiodides (I_3^- or I_5^-) from the cation is in a similar energy range as or higher than the barrier for the bond dissociation and ensued desorption of neutral iodine (I_2). This suggests that, instead of the physical diffusion of such a negatively charged multiatomic species, the exchange of neutral iodine (I_2) between the polyiodides can be an easier channel for the movement of polyiodide. For the transport of the monoiodide anion (I^-), we suggest the contribution of the Grotthuss-type ion exchange through the intermediately formed even-member anion (I_{2n}^-), in addition to drift and diffusion. As a result, we suggest that, instead of the commonly cited diffusion of the triiodide/iodide (I_3^-/I^-) redox couple, the exchange of neutral iodine (I_2) and the Grotthuss-type transport (I^-) constitute the dominant ion transport mechanism.

SECTION: Molecular Structure, Quantum Chemistry, and General Theory
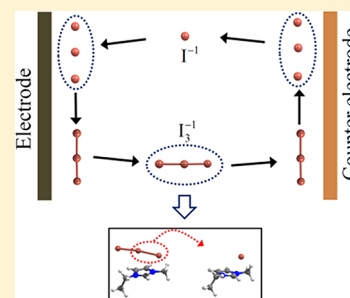
As energy storage-related devices, including rechargeable battery and solar cells,[1,2] become frontier topics of science, widespread efforts have been made to the improvement of known demerits of aqueous electrolytes. Besides the concerns about safety issues, organic solvents are vulnerable to evaporation, and thus have limited durability. In addition, the penetration of air and water vapors can lead to long-term instability of the device.[3,4] Therefore, the search for a nonflammable nonvolatile electrolyte is gaining great momentum, and many people have developed gel-type polymer electrolytes and ionic liquids (ILs).[5−9]

ILs are a class of liquid that is composed solely of cations, anions and their ion pairs. The potential of ILs for ionic current conduction has been attractive in various fields.[10] Usually two major objectives have been pursued: electrochemical stabilization and enhancement of the electrical conductivity of the electrolytes.[11] For example, in the case of dye-sensitized solar cells (DSSCs), ILs consisting of iodide anions have been used with various types of cations, such as 1-alkyl-3-alkylimidazolium.[12] In the perspective of stabilization of the electrolyte, the length of the alkyl chain has been controlled, eutectic melts have been used, or the inclusion of gelator has been tested.[11−14] Common concerns are about the conductance decrease incurred by such gelation. However, the literature has suggested an interesting possibility: In iodide-based electrolyte, the gelation or solidification may not necessarily degrade the conductivity.[12,13] The existence of neutral iodines (I_2) and longer iodide anions (I_{2n+1}^-) were suggested to be interrelated with the ionic conduction. However, their microscopic details have remained unknown.

During the DSSC operation, the iodide is oxidized at the working electrode surface donating electrons to the dye ($3I^- \rightarrow$

$I_3^- + 2e$) through certain intermediate states,[15,16] while being reduced at the counter electrode (CE) surface by getting electrons from the CE ($I_3^- + 2e \rightarrow 3I^-$). Overall, the longer iodide (I_3^-) and the short one (I^-) are equilibrated circulating the electric current. A few experimentalists discussed that the iodide ionic current cannot be simply attributed to the physical diffusion of the iodide ions (the movements of I_3^- and I^- in opposite directions).[17] Kawano et al. suggested that the limiting behavior of the ionic current has two components: one is due to the physical diffusion in proportion to the ion concentration, and the other is intuitively coined as an "exchange" mechanism, which scales as the square of the ion concentration.[18] Kubo et al. also suggested that a substantial part of the ionic current has contributions from nonphysical transport. Their Raman analysis showed that the formation of longer polyiodide can be correlated to the unexpected increase in the ionic conductance.[13] Recently, Thormølle et al. and Bai et al. studied the effect of iodine (I_2) concentration on conductivity in an IL and their eutectic melts, and suggested an iodine exchange, as a distinct mechanism from physical diffusion, that can lead to substantial contribution to the ion transport in the IL.[12,19]

However, the alleged iodine exchange mechanism and the effect of the polyiodide are not very rationalized. In the present work, we use first-principles computational methods to explore the microscopic details of iodine ion transport in electrolytes. We found, unlike the commonly cited diffusion of the I_3^-/I^- redox couple, the exchange of the neutral iodine (I_2) between polyiodides is the predominate mechanism: the overall ionic

current is conveyed by the diffusion/exchange of I^- and exchange of I_2. Using first-principles calculation methods, we calculated the binding strength between anions and 1-ethyl-3-methylimidazolium (EMI) cation and the bond dissociation energy of polyiodide. The calculated results indicate that the desorption barrier of the iodine molecule is smaller than the binding energy of the polyiodide onto the cation system.

We used the CAmbridge Serial Total Energy Package (CASTEP).[20] Ultrasoft pseudopotentials were used,[21] and the plane-wave basis set was used with the energy cutoff of 500 eV. The local density approximation (LDA) and the gradient-corrected Perdew–Burke–Ernzerhof (PBE) functional were employed to describe the electrons exchange-correlation potential.[22−24] For long-range van der Waals interaction and correction in energy, the Ortmann–Bechstedt–Schmidt (OBS) treatment is used to correct the LDA total energy, and the parameter-free Tkatchenko–Scheffler method is employed to correct the PBE total energy.[25,26] Hereafter, the dispersion force-corrected energetics are denoted as LDA-D and PBE-D, respectively. To cross-check the interaction energies between charged species, we also used the Gaussian 03 package (G03) for molecular geometries.[27] Møller–Plesset second-order perturbation (MP2) on the Hartree–Fock (HF) self-consistent field (SCF) were calculated with the 6-311G(d) basis set.[28,29] The geometry optimization in the CASTEP code was performed with using Broyden–Fletcher–Goldfarb–Shanno (BFGS) scheme until the total energy converged within 10^{-5} eV/atom with the maximum force being less than 0.03 eV/Å and with a maximum displacement less than 0.001 Å.[30] Transition states (TSs) were searched by the linear and quadratic synchronous transit method (LST/QST) implemented in CASTEP.[31]

Prior to the discussion of the exchange-mediated ion transfer mechanism, we investigated the binding strength between iodide and the cation. As a model for cations of the IL, EMI is chosen, as shown in Figure 1. In real experiments, the length of the alkyl chain of the cation is varied controlling the melting point, viscosity, and ion density.[11,12] For example, 1-ethyl-3-methylimidazolium iodide (EMII) and 1,3-dimethylimidazolium iodide (DMII) are solid at room temperature, whereas the melting point of 1-propyl-3-methylimidazolium iodide (PMII) is about −70 °C, and other imidazolium iodide ILs with longer alkyl chains are also liquid at room temperature.[12] In the present work, we instead took a shorter-length cation to simplify the model used in the computation. The Supporting Information (SI) contains results regarding PMII and confirms that the underlying physics suggested in this work does not much depend on the length of the alkyl chain. The binding strengths of I^-, I_3^-, and I_5^- onto the EMI cation were found to be 2.43, 1.94, and 1.87 (1.68/1.88, 1.62/1.8 and 1.46/1.76) eV, respectively, in the MP2 (LDA-D/PBE-D) results. Throughout this work, the iodide–EMI complexes are denoted by EMII, $EMII_3$, and $EMII_5$, respectively, as shown in Figure 1a−c. All the computations were performed with the spin singlet configuration. The energy references are taken from the isolated optimized cation and anions. The closest interatomic distances between iodides and EMI, as denoted by dashed lines in Figure 1a, b, and c, are 3.11, 3.16, and 3.06 Å, respectively. The longer polyiodide has the weaker binding strength per iodide onto the EMI cation. This can be attributed to the nature of Coulombic interaction. In the case of longer polyiodides, the extra electron charge ($-e$) of the anions is more delocalized than the cases of smaller iodides, resulting in a
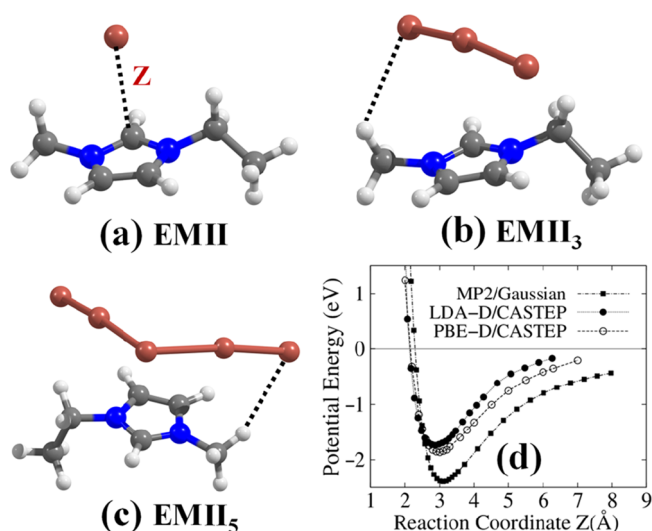

Figure 1. The optimized geometries of (a) I^-, (b) I_3^-, and (c) I_5^- onto the EMI cation, denoted as EMII, $EMII_3$, and $EMII_5$, respectively. (d) The potential energy curve of I^- from EMI. For Gaussian work, the energy reference is taken from the isolated cation and anion. For CASTEP, the energy references are taken from the supercell calculation in which the cation and anions are largely separated. Blue, gray, brown, and small white balls representing nitrogen, carbon, iodine, and hydrogen atom, respectively. The dashed line indicates the closest distance between the iodides and EMI.

weaker Coulombic attraction toward the positively charged EMI.

We also investigated the desorption behaviors of iodide anions from the EMI cation. In Figure 1d, the iodide is rigidly displaced along the optimized C−I bond direction, as denoted by the dashed line in Figure 1a. At a distance larger than 4 Å, the curve shows a good fitting to the inverse of the distance, revealing the nature of the Coulombic attraction. It is noteworthy that even at a distance of about 6.3 Å, the interaction between the EMI cation and I^- is quite substantial (ca. −0.7, −0.17, and −0.35 eV in MP2, LDA-D and PBE-D result, respectively). The Mullikan charge analysis of the two ions at various separations indeed indicates that the cation and the anion parts are close to singly charged ions. The cases of desorption of polyiodide (I_3^- or I_5^-) on EMI cation also showed similar long-range behaviors (not shown). The potential energy curve of iodide during desorption from PMI, as shown in Figure S1a (SI), indicates the same trend of Coulombic interaction. In real materials, the screening effect can mitigate such Coulombic tails between ion pairs. However, the intermolecular distances between the anion and cation, in the bonding configuration shown in Figure 1, are about 3 Å, and the binding mechanism is not much affected by the screening effect.

The potential energy curves, calculated by the LDA-D and PBE-D, for desorption of neutral I_2 from the $EMII_3$ configuration are shown in the Figure 2a. Since the iodine (I_2) is neutral, the curve does not show a Coulombic tail. It is found that when the I_2 is separated from the remaining iodide by about 6 Å, the interaction is almost negligible. The energy cost mostly originated from the bond breaking from the triiodide on EMI. It is important to note that the depth of the potential well, shown in Figure 2a, is smaller to that of binding energy of triiodide onto EMI. This suggests that the bond breaking of the triiodide and the ensued desorption of I_2
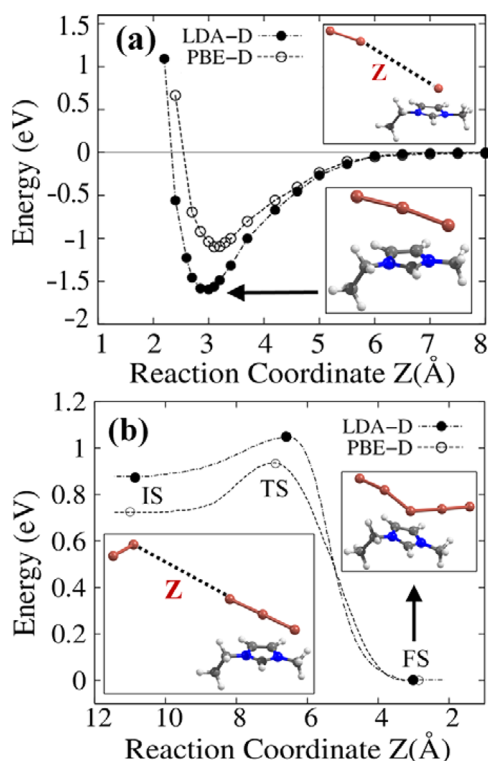
Figure 2. The potential energy curve for the desorption of neutral I_2 from the ion pairs of (a) triiodide (I_3^-), (b) polyiodide (I_5^-), and EMI. Insets show the optimized geometries and indicate the reaction coordinate that is the distance between I_2 and remaining iodide, as indicated by Z. For panel a, the energy reference is of largely separated I_2 and EMII. For b, the energy is with respect to FS. The dash-dotted line is only a guide to the eye.

Figure 3. The barrier for I_2 movement from $EMII_5$ to EMII. (a) The optimized geometry of IS and FS. (b) The energy barrier as a function of the distance (D) between two EMIs. Inset on the right shows the definition of the barrier. Inset on the left shows the TS geometry calculated with $D = 7.0$ Å. EMIs are not shown for clarity. The dash-dotted line is only a guide to the eye.

expends less energy cost than the full desorption of the triiodide from the cation sites. The desorption of neutral iodine from $PMII_3$ is in Figure S1b. The cases of PMII also show similar energetics as those of EMII.

We also performed the same investigation with I_5^-, as shown in Figure 2b. The full separation of I_5^- from EMI costs 1.46 and 1.76 eV in the LDA-D and PBE-D, respectively (see the previous paragraph regarding Figure 1c). However, the bond breaking ($I_5^- \rightarrow I_3^- + I_2$) and ensued desorption of neutral I_2 required a lower energy cost (1.07 and 0.93 eV with LDA-D and PBE-D, respectively), the energy difference between the TS and final state (FS) in Figure 2b. Mulliken analysis showed that, on the EMI, the triiodide is almost singly negatively charged.[32] The migration of neutral I_2 after the bond breaking would not be interrupted by the long-range Coulombic potentials, and thus, can be more mobile than heavier charged polyiodides, effectively contributing to the density equilibrium between iodide anions. It is noteworthy that there is a small barrier in the formation of $EMII_5$ from $EMII_3$ and neutral I_2; for example, in the PBE-D result, the energy difference between the TS and initial state (IS) is about 0.2 eV, as shown in Figure 2b. This is attributed to the closed-shell nature of I_3^-, whose electronic structure is a bit resistive in the formation of longer polyiodide.

Desorption and readsorption of I_2 can effectively relocate the polyiodides in the electrolyte. We now investigate the exchange mechanism of I_2 in the iodide−EMI pairs. In Figure 3, we calculate the transport of I_2 from $EMII_5$ to EMII, finally resulting in two $EMII_3$, with variable distances between two EMI cations. The optimized geometries of the IS and FS are
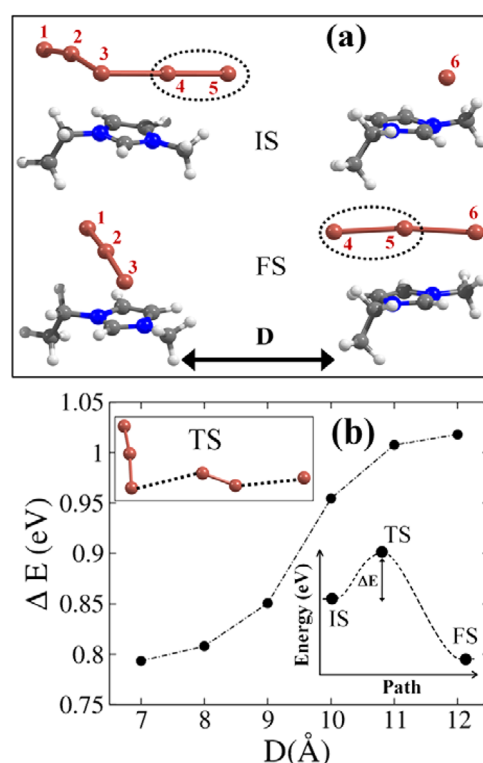
shown in Figure 3a. The dotted circle indicates the iodine dimer to be exchanged during the process. To investigate the effect of the ion density, the dependence of the energy barriers (ΔE) on the distance between EMIs were calculated, as shown in Figure 3b. The barrier height is defined here as the height from IS to TS. In the literature, the average separations between ion species were estimated to be 8 Å for about 0.5 M solution of iodide solution[13,33] and more recently about 3.9 M I_2 in 5.6 M PMII as electrolyte has been reported.[34] We observe that, as the distance between two EMI decreases, the barrier for the I_2 movement substantially decreases, leading to a higher conductivity, consistent with the experimental results.[18,19] The curve indicate that, for a large distance D, the barrier height is almost the same as the barrier height of I_2 desorption from $EMII_5$ (1.02 eV, as shown in Figure 2b). In the opposite limit of high density (closer distance between EMIs) the barrier height converges to be about 0.79 eV.

In previous paragraphs, we showed that movement of polyiodides can be effectively mediated by the exchange of neutral iodine molecules. This explains the dominant microscopic mechanism for the triiodide (or polyiodide) transport from the working electrode to the CE. We now consider the transport of iodide (I^-) that is believed to be generated at the surface of the CE. The movement of the iodide through the overall charge neutral IL can substantially be contributed by the drift motion derived by the external field. However, here we suggest that the microscopic motion, especially in the presence of polyiodides, can accompany the Grotthus-type ion exchange. The schematic description of our model is shown in Figure 4. The most favorable adsorption site of I^- onto $EMII_3$ is just the
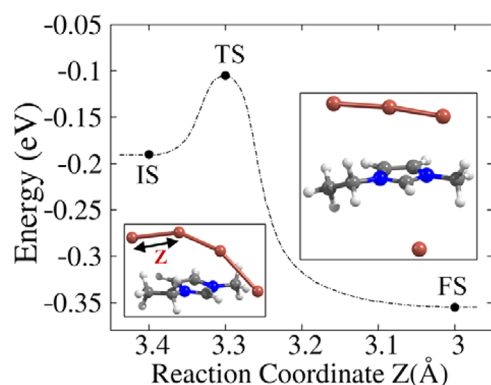
Figure 4. The energy barrier curve for the iodide approaching toward EMII$_3$ and inset shows the relaxed structure of IS and FS. TS represent the transition state. The energies are referenced to largely separated I$^-$ and EMII$_3$. The dash-dotted line is only a guide to the eye.

side opposite to the triiodide, as depicted by the FS in the inset of Figure 4. Our total energy minimization calculation showed that the chained four iodide (I$_4$) can also sit on the EMI, as indicated with IS in the inset of Figure 4. Mulliken charge analysis revealed that the four-membered iodide is almost doubly charged: I$_4^{2-}$. The exothermic reaction energy from IS to FS is found to be about 0.16 eV. The estimated bond length between the first and second and between the third and fourth iodine of I$_4^{2-}$ is longer than 3.1 Å (IS of Figure 4). This signifies clearly that the EMII$_4^-$ is not in a very stable state. The depth of the potential well of both the IS (0.19 eV) and FS (0.35 eV), with respect to the completely separated EMII$_3$ and I$^-$, is very low. This suggests that both the IS and FS can exist only transiently, contributing to the iodide flow: through the possible exchange of the iodide (I$^-$) between IS and FS in Figure 4. In a sense, this type of iodide transport through the intermediately formed EMII$_4^-$ is reminiscent of the Grotthuss-type proton exchange in the water network: the combination into EMII$_4^-$ and separation into EMII$_3$ and I$^-$ can effectively result in the transport of the charged ion.

We also investigated the possibility of iodide hopping into EMII. However, our total energy results revealed that the EMII$_2^-$ system is not stable, even locally, as shown in the Figure S2: the two iodides are far separated from each other either on the same side or the opposite side of EMI cation. This indicates that the Columbic repulsion between iodides (the two I$^-$) is strong, and thus, the hopping through the EMII$_2^-$ is forbidden.

In summary, we investigated the underlying energetics related to the behaviors of anions and I$_2$ in iodide IL using first-principles calculations. Unlike the conventional understanding that states the flow of I$_3^-$ from working electrode to CE, our results suggested that the exchange of neutral iodide (I$_2$) between polyiodides can be a more dominant mechanism than the physical diffusion of I$_3^-$. We suggested that the flow of iodide (I$^-$) from the CE to the working electrode, through drift and diffusion, can also have a substantial contribution from the Grotthuss-like ion exchange mechanism. This exchange mechanism of iodine (I$_2$) and iodide (I$^-$) explains the role and importance of the presence of neutral iodine (I$_2$) and longer iodide chains.

■ ASSOCIATED CONTENT

ⓢ Supporting Information

The potential energies of iodides on 1-propyl-3-methylimidazolium (PMI), which has longer alkyl chain, and lower melting point, are presented. This material is available free of charge via the Internet at http://pubs.acs.org.

■ AUTHOR INFORMATION

Corresponding Author

*E-mail: noejung@unist.ac.kr.

Notes

The authors declare no competing financial interest.

■ ACKNOWLEDGMENTS

■ REFERENCES

(1) Chakrapani, V.; Rusli, F.; Filler, M. A.; Kohl, P. A. Quaternary Ammonium Ionic Liquid Electrolyte for a Silicon Nanowire-Based Lithium Ion Battery. *J. Phys. Chem. C* **2011**, *115*, 22048−22053.

(2) Jeon, J.; Kim, H.; Goddard, W. A.; Pascal, T. A.; Lee, G.-I.; Kang, J. K. The Role of Confined Water in Ionic Liquid Electrolytes for Dye Sensitized Solar Cells. *J. Phys. Chem. Lett.* **2012**, *3*, 556−559.

(3) Kay, A.; Grätzel, M. Low Cost Photovoltaic Modules Based on Dye Sensitized Nanocrystalline Titanium Dioxide and Carbon Powder. *Sol. Energy Mater. Sol. Cells* **1996**, *44*, 99−117.

(4) Li, D.; Qin, D.; Deng, M.; Luo, Y.; Meng, Q. Optimization the Solid-State Electrolytes for Dye-Sensitized Solar Cells. *Energy Env. Sc.* **2009**, *2*, 283−291.

(5) Tang, C.; Hackenberg, K.; Fu, Q.; Ajayan, P. M.; Ardebili, H. High Ion Conducting Polymer Nanocomposite Electrolytes Using Hybrid Nanofillers. *Nano Lett.* **2012**, *12*, 1152−1156.

(6) Chen, J.-G.; Liu, K.-Y.; Chen, C.-Y.; Lin, C.-Y.; Huang, K.-C.; Lai, Y.-H.; Wu, C-G; Lin, K.-F.; Ho, K.-C. Efficient Gel-Type Electrolyte with Bismaleimide via In Situ Low Temperature Polymerization in Dye-Sensitized Solar Cells. *J. Polym. Sci., Part A: Polym. Chem.* **2010**, *48*, 4950−4957.

(7) Bailey, M. M.; Townsend, M. B.; Jernigan, P. L.; Sturdivant, J.; Hough-Troutman, W. L.; Rasco, J. F.; Swatloski, R. P.; Rogers, R. D.; Hood, R. D. Developmental Toxicity Assessment of the Ionic Liquid 1-Butyl-3-Methylimidazolium Chloride in CD-1 Mice. *Green Chem.* **2008**, *10*, 1213−1217.

(8) Ghatee, M. H.; Zolghadr, A. R; Moosavi, F.; Ansari, Y. Studies of Structural, Dynamical, and Interfacial Properties of 1-Alkyl-3-Methylimidazolium Iodide Ionic Liquids by Molecular Dynamics Simulation. *J. Chem. Phys.* **2012**, *136*, 124706.

(9) Singh, P. K; Bhattacharya, B.; Nagarale, R. K.; Pandey, S. P.; Kim, K. W.; Rhe, H.-W. Ionic Liquid Doped Poly(*N*-methyl 4-vinylpyridine iodide) Solid Polymer Electrolyte for Dye-Sensitized Solar Cell. *Synth. Met.* **2010**, *160*, 950−954.

(10) Bridges, N. J.; Rogers, R. D. Can Kosmotropic Salt/Chaotropic Ionic Liquid (Salt/Salt Aqueous Biphasic Systems) Be Used to Remove Pertechnetate from Complex Salt Waste? *Sep. Sci. Technol.* **2008**, *43*, 1083−1090.

(11) Castner, E. W., Jr.; Wishart, J. F. Spotlight on Ionic Liquids. *J. Chem. Phys.* **2010**, *132*, 120901.

(12) Bai, Y.; Cao, Y.; Zhang, J.; Wang, M.; Li, R.; Wang, P.; Zakeeruddin, S. M.; Grätzel, M. High-Performance Dye-Sensitized Solar Cells Based on Solvent-Free Electrolytes Produced from Eutectic Melts. *Nat. Mater.* **2008**, *7*, 626−630.

(13) Kubo, W.; Murakoshi, K.; Kitamura, T.; Yoshida, S.; Haruki, M.; Hanabusa, K.; Shirai, H.; Wada, Y.; Yanagida, S. Quasi-Solid-State Dye-Sensitized TiO_2 Solar Cells: Effective Charge Transport in Mesoporous Space Filled with Gel Electrolytes Containing Iodide and Iodine. *J. Phys. Chem. B.* **2001**, *105*, 12809−12815.

(14) Yoon, J.; Kang, D. K.; Won, J.; Park, J.-Y.; Kang, Y. S. Dye-Sensitized Solar Cells Using Ion-Gel Electrolytes for Long-Term Stability. *J. Power Sources* **2012**, *201*, 395−401.

(15) Boschloo, G.; Hagfeldt, A. Characteristics of the Iodide/Triiodide Redox Mediator in Dye-Sensitized Solar Cells. *Acc. Chem. Res.* **2009**, *42*, 1819−1826.

(16) Rowley, J. G.; Farnum, B. H.; Ardo, S.; Meyer, G. J. Iodide Chemistry in Dye-Sensitized Solar Cells: Making and Breaking I−I Bonds for Solar Energy Conversion. *J. Phys. Chem. Lett.* **2010**, *1*, 3132−3140.

(17) Papageorgiou, N.; Athanassov, Y.; Armand, M.; BonhGte, P.; Pettersson, H.; Azam, A.; Grätzel, M. The Performance and Stability of Ambient Temperature Molten Salts for Solar Cell Applications. *J. Electrochem. Soc.* **1996**, *143*, 3099−3108.

(18) Kawano, R.; Watanabe, M. Equilibrium Potentials and Charge Transport of an I^-/I_3^- Redox Couple in an Ionic Liquid. *Chem. Commun.* **2003**, 330−331.

(19) Thorsmølle, V. K.; Rothenberger, G.; Topgaard, D.; Brauer, J. C.; Kuang, D.-B.; Zakeeruddin, S. M.; Lindman, B.; Grätzel, M.; Moser, J.-E. Extraordinarily Efficient Conduction in a Redox-Active Ionic Liquid. *Chem. Phys. Chem.* **2011**, *12*, 145−149.

(20) Segall, M. D.; Lindan, P. L. D.; Probert, M. J.; Pickard, C. J.; Hasnip, P. J.; Clark, S. J.; Payne, M. C. First-Principles Simulation: Ideas, Illustrations and the CASTEP Code. *J. Phys.: Condens. Matter* **2002**, *14*, 2717−2744.

(21) Vanderbilt, D. Soft Self-Consistent Pseudopotentials in a Generalized Eigenvalue Formalism. *Phys. Rev. B* **1990**, *41*, 7892−7895.

(22) Perdew, J. P.; Zunger, A. Self-Interaction Correction to Density-Functional Approximations for Many-Electron Systems. *Phys. Rev. B* **1981**, *23*, 5048−5079.

(23) Ceperley, D. M.; Alder, B. J. Ground State of the Electron Gas by a Stochastic Method. *Phys. Rev. Lett.* **1980**, *45*, 566−569.

(24) Perdew, J. P.; Burke, K.; Ernzerhof, M. Generalized Gradient Approximation Made Simple. *Phys. Rev. Lett.* **1996**, *77*, 3865−3868.

(25) Ortmann, F.; Bechstedt, F.; Schmidt, W. G. Semiempirical van der Waals Correction to the Density Functional Description of Solids and Molecular Structures. *Phys. Rev. B* **2006**, *73*, 205101.

(26) Tkatchenko, A.; Scheffler, M. Accurate Molecular van der Waals Interactions from Ground-State Electron Density and Free-Atom Reference Data. *Phys. Rev. Lett.* **2009**, *102*, 073005.

(27) Frisch, M. J.; Trucks, G. W.; Schlegel, H. B.; Scuseria, G. E.; Robb, M. A.; Cheeseman, J. R.; et al. *Gaussian 03*, revision C.02; Gaussian, Inc: Wallingford, CT, 2004.

(28) Møller, C.; Plesset, M. S. Note on an Approximation Treatment for Many-Electron Systems. *Phys. Rev.* **1934**, *46*, 618.

(29) Krishnan, R.; Binkley, J. S.; Seeger, R.; Pople, J. A. Self-Consistent Molecular Orbital Methods. XX. A Basis Set for Correlated Wave Functions. *J. Chem. Phys.* **1980**, *72*, 650−654.

(30) Pfrommer, B. G.; Cote, M.; Louie, S. G.; Cohen, M. L. Relaxation of Crystals with the Quasi-Newton Method. *J. Comput. Phys.* **1997**, *131*, 233−240.

(31) Govind, N.; Petersen, M.; Fitzgerald, G.; K-Smith, D.; Andzelm, J. A Generalized Synchronous Transit Method for Transition State Location. *Comput. Mater. Sci.* **2003**, *28*, 250−258.

(32) Braïda, B.; Hiberty, P. C. What Makes the Trifluoride Anion F_3^- So Special? A Breathing-Orbital Valence Bond Ab Initio Study. *J. Am. Chem. Soc.* **2004**, *126*, 14890−14898.

(33) Turro, N. J. *Modern Molecular Photochemistry*; The Benjamin/Cummings Publishing Company, Inc.: Menlo Park, CA, 1978; p 319.

(34) Thorsmølle, V. K.; Topgaard, D.; Brauer, J. C.; Zakeeruddin, S. M.; Lindman, B.; Grätzel, M.; Moser., J.-E. Conduction Through Viscoelastic Phase in a Redox-Active Ionic Liquid at Reduced Temperatures. *Adv. Mater.* **2012**, *24*, 781−784.